Theory of total-internal-reflection tomography

P. Scott Carney

Department of Electrical and Computer Engineering, University of Illinois at Urbana-Champaign, Urbana, Illinois 61821

John C. Schotland*

Department of Electrical Engineering, Washington University, St. Louis, Missouri 63130

Received June 20, 2002; revised manuscript received October 30, 2002; accepted November 19, 2002

A method is presented to reconstruct three-dimensional tomographic images of weakly scattering objects with subwavelength resolution. The method may be applied to data available in phase-sensitive, total-internal-reflection microscopy. The results follow from an analysis of the near-field inverse scattering problem with evanescent waves. © 2003 Optical Society of America

OCIS codes: 290.3200, 180.6900, 100.6950.

1. INTRODUCTION

Total-internal-reflection microscopy (TIRM) brings to conventional microscopy the added functionality of illumination by evanescent waves. Incorporation of evanescent waves in the illuminating field is an important development for several reasons. First, the exponential decay of such waves along one direction allows for the control of the depth of penetration of the illuminating field. Second, evanescent waves may be used to resonantly excite surface plasmon modes of the sample. Finally, and perhaps most important, evanescent waves may be employed to supersede the Rayleigh diffraction limit of order half the wavelength, $\lambda/2$.

TIRM has been in practical use for decades. It has been employed primarily as a surface inspection technique,[1,2] though the sensitivity of the field to distance along the decay axis has been used to advantage in applications such as the measurement of distance between two surfaces.[3] Until recently the opportunities for transverse superresolution made possible by the high spatial-frequency content of the probe field have been largely overlooked. However, advances in the realization of superresolved imaging using TIRM have been reported recently in the literature. A direct imaging approach resulting from the marriage of standing-wave illumination techniques and TIRM has been described[4] that achieves transverse resolution of $\lambda/7$. An additional approach has been brought forward in which structural information derived from a scattering object is extracted from the scattered field and a three-dimensional reconstruction of the object is made.[5] This requires an understanding of the information content of the TIRM experiment, which was recently obtained for the case of weakly scattered fields.[6,7] The reconstruction is accomplished by making use of an analytic solution to the inverse scattering problem with evanescent waves.[5] This method is called total-internal-reflection tomography (TIRT).

TIRT offers several advantages over existing modalities for three-dimensional microscopy. First, the evanescent waves used for illumination encode the subwavelength structure of the scattering object on the scattered field. It is thus possible to obtain subwavelength-resolved images of the sample as is done in other near-field techniques, such as near-field scanning optical microscopy (NSOM),[8–12] without the technical difficulties encountered with probe–sample interactions. Second the results of the reconstruction are unambiguous in the sense that the relation between the scattered field and the three-dimensional structure of the sample, as described by the spatial dependence of the susceptibility, is made manifest. This is somewhat analogous to the transition from projection radiography to computed tomography.

In this paper the results presented in Ref. 5 are expanded to include effects significant for experimental realization. In Section 2 the forward problem of scattering of evanescent scalar and vector wave fields from a sample characterized by the dielectric susceptibility is formulated. The illuminating evanescent waves are assumed to be generated at the interface of two half-spaces of different indices of refraction. For this reason boundary conditions on the scattered field are taken into account. In Section 3 these results are used to obtain the solution to the corresponding inverse scattering problems. The results are discussed in Section 4.

2. FORWARD PROBLEM

In this section the scattering of evanescent waves from weakly scattering dielectric media is considered. Scalar waves are treated first. The scalar field is of independent importance as it bears on problems in acoustics and quantum mechanics. To treat problems in optical microscopy, it is necessary to consider the electromagnetic (vector) theory of scattering to account for the effects of polarization. Note that the vector theory is essential since the scalar approximation to the scattering of electromagnetic waves is invalid when the dielectric susceptibility varies on subwavelength scales.

1084-7529/2003/030542-06$15.00

A. Scalar Case

Consider an experiment in which a monochromatic scalar field is incident on a dielectric medium with susceptibility $\eta(\mathbf{r})$. The field incident on the sample will be taken to be an evanescent wave which is generated by total internal reflection at the interface of two half-spaces. One half-space, taken to be $z \geqslant 0$, will have the vacuum index of refraction 1 while the $z < 0$ half-space will have an index of refraction n. The situation is illustrated in Fig. 1. The scalar field $U(\mathbf{r})$ obeys the reduced wave equation

$$\nabla^2 U(\mathbf{r}) + k_0{}^2 n^2(z) U(\mathbf{r}) = -4\pi k_0{}^2 \eta(\mathbf{r}) U(\mathbf{r}), \quad (1)$$

where k_0 is the free-space wave number, $n(z)$ is the z-dependent index of refraction as described above, and the support of $\eta(\mathbf{r})$ is contained in the $z \geqslant 0$ half-space. The total field may be written as the sum

$$U = U_i + U_s, \quad (2)$$

where U_i and U_s represent the incident and scattered fields, respectively. The incident field obeys the homogeneous equation

$$\nabla^2 U_i(\mathbf{r}) + k_0{}^2 n^2(z) U_i(\mathbf{r}) = 0. \quad (3)$$

The scattered field obeys the equation

$$\nabla^2 U_s(\mathbf{r}) + k_0{}^2 n^2(z) U_s(\mathbf{r}) = -4\pi k_0{}^2 \eta(\mathbf{r}) U(\mathbf{r}). \quad (4)$$

Equation (4) may be recast as the integral equation

$$U_s(\mathbf{r}) = k_0{}^2 \int \mathrm{d}^3 r' G(\mathbf{r}, \mathbf{r}') U(\mathbf{r}') \eta(\mathbf{r}'), \quad (5)$$

where $G(\mathbf{r}, \mathbf{r}')$ is the Green's function.

The Green's function $G(\mathbf{r}, \mathbf{r}')$ satisfies the equation

$$\nabla^2 G(\mathbf{r}, \mathbf{r}') + n^2(z) k_0{}^2 G(\mathbf{r}, \mathbf{r}') = -4\pi\delta(\mathbf{r} - \mathbf{r}'), \quad (6)$$

and, because the field and its normal derivative must be continuous, obeys the boundary conditions

$$G(\mathbf{r}, \mathbf{r}')|_{z=0^+} = G(\mathbf{r}, \mathbf{r}')|_{z=0^-}; \quad (7)$$

$$\hat{\mathbf{z}} \cdot \nabla G(\mathbf{r}, \mathbf{r}')|_{z=0^+} = \hat{\mathbf{z}} \cdot \nabla G(\mathbf{r}, \mathbf{r}')|_{z=0^-}. \quad (8)$$

It may be seen that $G(\mathbf{r}, \mathbf{r}')$ admits the plane-wave decomposition

$$G(\mathbf{r}, \mathbf{r}') = \frac{i}{2\pi} \int \frac{\mathrm{d}^2 q}{k_z(\mathbf{q})} \{1 + R(\mathbf{q}) \exp[2ik_z(\mathbf{q})z']\} \times \exp[i\mathbf{k}(\mathbf{q}) \cdot (\mathbf{r} - \mathbf{r}')], \quad (9)$$

where $R(\mathbf{q})$ is the reflection coefficient given by

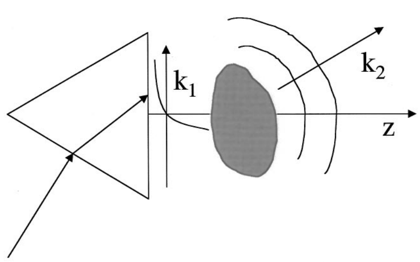

Fig. 1. Illustration of the measurement scenario: Evanescent waves are generated at the prism face by total internal reflection (TIR); the TIR is then partly frustrated by the presence of the scatterer, which scatters evanescent modes to homogeneous modes that propagate to the far zone.

$$R(\mathbf{q}) = \frac{k_z(\mathbf{q}) - k_z{}'(\mathbf{q})}{k_z(\mathbf{q}) + k_z{}'(\mathbf{q})}, \quad (10)$$

with

$$k_z(\mathbf{q}) = (k_0{}^2 - q^2)^{1/2}, \quad (11)$$

$$k_z{}'(\mathbf{q}) = (n^2 k_0{}^2 - q^2)^{1/2}, \quad (12)$$

and $\mathbf{k}(\mathbf{q}) = [\mathbf{q}, k_z(\mathbf{q})]$. The plane-wave modes appearing in Eq. (7) are labeled by the transverse part of the wave vector $\mathbf{q}$. The modes for which $|\mathbf{q}| \leqslant k_0$ correspond to propagating waves while the modes with $|\mathbf{q}| > k_0$ correspond to evanescent waves. In the limit that $n(z) = 1$, the reflection coefficient R vanishes and Eq. (9) yields the usual free-space Green's function.

The incident field is taken to be an evanescent plane wave of the form

$$U_i(\mathbf{r}) = \exp[i\mathbf{k}(\mathbf{q}) \cdot \mathbf{r}], \quad (13)$$

where $\mathbf{q}$ labels the transverse part of the incident wave vector. If the evanescent wave is generated by a prism with index of refraction n, then $k_0 \leqslant |\mathbf{q}| \leqslant nk_0$. Thus k_z is imaginary with the choice of sign dictated by the physical requirement that the field decay exponentially with increasing values of z. Within the accuracy of the first Born approximation, the total field may be replaced by the incident field in the right-hand side of Eq. (4) and the expression for the scattered field is obtained as

$$U_s(\mathbf{r}) = k_0{}^2 \int \mathrm{d}^3 r' G(\mathbf{r}, \mathbf{r}') U_i(\mathbf{r}') \eta(\mathbf{r}'). \quad (14)$$

In the far zone of the scatterer, the leading term in the asymptotic expansion of the Green's function is given by the expression

$$G(\mathbf{r}, \mathbf{r}') \sim \{1 + R(\mathbf{q}) \exp[2ik_z(\mathbf{q})z']\} \times \frac{\exp(ik_0 r)}{r} \exp[-i\mathbf{k}(\mathbf{q}) \cdot \mathbf{r}'], \quad (15)$$

where $\mathbf{k}(\mathbf{q})$ is parallel to $\mathbf{r}$ and $|\mathbf{q}| \leqslant k_0$. Using this result and expression (14) it is found that the scattered field behaves as an outgoing homogeneous wave of the form

$$U_s(\mathbf{r}) \sim \frac{\exp(ik_0 r)}{r} A(\mathbf{q}_1, \mathbf{q}_2), \quad (16)$$

where $\mathbf{q}_1$ and $\mathbf{q}_2$ are the transverse parts of the incident and outgoing wave vectors, respectively. Here $A(\mathbf{q}_1, \mathbf{q}_2)$—which is the scattering amplitude associated with the scattering of evanescent plane waves with transverse wave vector $\mathbf{q}_1$ into homogeneous plane waves with transverse wavevector $\mathbf{q}_2$—is related to the susceptibility of the scattering object by the expression

$$A(\mathbf{q}_1, \mathbf{q}_2) = k_0^2 \int \mathrm{d}^3 r \{1 + R(\mathbf{q}_2) \exp[2ik_z(\mathbf{q}_2)z]\} \times \exp\{i[\mathbf{k}(\mathbf{q}_1) - \mathbf{k}(\mathbf{q}_2)] \cdot \mathbf{r}\} \eta(\mathbf{r}). \quad (17)$$

This is the observable quantity of interest. The inversion of this integral equation to obtain $\eta(\mathbf{r})$ will be addressed in Subsection 3.A.

B. Vector Case

In order to treat properly the scattering of optical fields, it is necessary to consider the vector theory of electromagnetic scattering. As illustrated in Fig. 1, an evanescent wave is incident on a dielectric medium with susceptibility $\eta(\mathbf{r})$, and it is assumed that the evanescent wave is produced at the interface of two half-spaces. Only nonmagnetic materials are considered. Accordingly, the magnetic field need not be taken into account and only the electric field will be needed. The electric field $\mathbf{E}$ satisfies the reduced wave equation

$$\nabla \times \nabla \times \mathbf{E}(\mathbf{r}) - k_0^2 n^2(z) \mathbf{E}(\mathbf{r}) = 4\pi k_0^2 \eta(\mathbf{r}) \mathbf{E}(\mathbf{r}), \quad (18)$$

where k_0 is the free-space wave number and $n(z)$ is the background index of refraction as described in Subsection 2.A. The field is decomposed into the sum of two parts

$$\mathbf{E} = \mathbf{E}^i + \mathbf{E}^s. \quad (19)$$

The incident field $\mathbf{E}^i$ obeys the homogeneous equation

$$\nabla \times \nabla \times \mathbf{E}^i(\mathbf{r}) - k_0^2 n^2(z) \mathbf{E}^i(\mathbf{r}) = 0. \quad (20)$$

The scattered field $\mathbf{E}^s$ obeys the equation

$$\nabla \times \nabla \times \mathbf{E}^s(\mathbf{r}) - k_0^2 n^2(z) \mathbf{E}^s(\mathbf{r}) = 4\pi k_0^2 \eta(\mathbf{r}) \mathbf{E}(\mathbf{r}). \quad (21)$$

Equation (21) may be reformulated as the integral equation

$$E^s_\alpha(\mathbf{r}) = k_0^2 \int \mathrm{d}^3 r' G_{\alpha\beta}(\mathbf{r}, \mathbf{r}') E_\beta(\mathbf{r}') \eta(\mathbf{r}'), \quad (22)$$

where $G_{\alpha\beta}(\mathbf{r}, \mathbf{r}')$ is the Green's tensor for the half-space and the summation convention over repeated indices applies and will apply throughout.

The Green's tensor $G_{\alpha\beta}(\mathbf{r}, \mathbf{r}')$ satisfies the equation

$$\nabla \times \nabla \times \mathbf{G}(\mathbf{r}, \mathbf{r}') - k_0^2 n^2(z) \mathbf{G}(\mathbf{r}, \mathbf{r}') = 4\pi \delta(\mathbf{r} - \mathbf{r}') \mathbf{I}, \quad (23)$$

where $\mathbf{I}$ is the unit tensor. The Green's tensor must also satisfy the boundary conditions

$$\hat{\mathbf{z}} \times \mathbf{G}(\mathbf{r}, \mathbf{r}')|_{z=0^+} = \hat{\mathbf{z}} \times \mathbf{G}(\mathbf{r}, \mathbf{r}')|_{z=0^-}, \quad (24)$$

$$\hat{\mathbf{z}} \times \nabla \times \mathbf{G}(\mathbf{r}, \mathbf{r}')|_{z=0^+} = \hat{\mathbf{z}} \times \nabla \times \mathbf{G}(\mathbf{r}, \mathbf{r}')|_{z=0^-}. \quad (25)$$

Making use of a plane-wave decomposition, it may be found that[13,14]

$$G_{\alpha\beta}(\mathbf{r}, \mathbf{r}') = \frac{i}{2\pi} \int \frac{\mathrm{d}^2 q}{k_z(\mathbf{q})} g_{\alpha\beta}(\mathbf{q}, z) \exp[i\mathbf{k}(\mathbf{q}) \cdot (\mathbf{r} - \mathbf{r}')]. \quad (26)$$

where it is assumed that $z > z' > 0$. The explicit form of g is given in Appendix A.

The incident field is an evanescent plane wave with polarization $\mathbf{E}^{(0)}$

$$E^i_\alpha(\mathbf{r}) = E^{(0)}_\alpha \exp[i\mathbf{k}(\mathbf{q}) \cdot \mathbf{r}], \quad (27)$$

where $\mathbf{k}(\mathbf{q})$ is the incident wave vector and $k_0 \leqslant |\mathbf{q}| \leqslant nk_0$. Within the accuracy of the first Born approximation, the scattered field is given by the expression

$$E^s_\alpha(\mathbf{r}) = k_0^2 \int \mathrm{d}^3 r' G_{\alpha\beta}(\mathbf{r}, \mathbf{r}') E^{(0)}_\beta \exp[i\mathbf{k}(\mathbf{q}) \cdot \mathbf{r}'] \eta(\mathbf{r}'). \quad (28)$$

In the far zone of the scatterer the Green's tensor assumes the asymptotic form

$$G_{\alpha\beta}(\mathbf{r}, \mathbf{r}') \sim g_{\alpha\beta}(\mathbf{q}, z) \frac{\exp(ik_0 r)}{r} \exp[-i\mathbf{k}(\mathbf{q}) \cdot \mathbf{r}'], \quad (29)$$

where $\mathbf{k}(\mathbf{q})$ lies in the direction of $\mathbf{r}$. Thus the scattered field becomes

$$E^s_\alpha(\mathbf{r}) \sim A_{\alpha\beta}(\mathbf{q}_1, \mathbf{q}_2) E^{(0)}_\beta \frac{\exp(ik_0 r)}{r}, \quad (30)$$

where $\mathbf{q}_1$ and $\mathbf{q}_2$ are the transverse parts of the of incident and outgoing wave vectors, respectively. $A_{\alpha\beta}(\mathbf{q}_1, \mathbf{q}_2)$ denotes the tensor scattering amplitude which is related to the susceptibility by the expression

$$A_{\alpha\beta}(\mathbf{q}_1, \mathbf{q}_2) = \int \mathrm{d}^3 r w_{\alpha\beta}(\mathbf{q}_2, z) \times \exp\{i[\mathbf{k}(\mathbf{q}_1) - \mathbf{k}(\mathbf{q}_2)] \cdot \mathbf{r}\} \eta(\mathbf{r}), \quad (31)$$

where

$$w_{\alpha\beta}(\mathbf{q}, z) = k_0^2 g_{\alpha\beta}(\mathbf{q}, z). \quad (32)$$

Inversion of the above integral equation to obtain $\eta(\mathbf{r})$ will be discussed in Subsection 3.B.

3. INVERSE PROBLEM

The inverse problem consists of reconstructing the susceptibility from measurements of the scattering amplitude. To this end it is desirable to construct the pseudoinverse solution of the integral Eqs. (17) and (31). The method of singular value decomposition (SVD) provides a means to obtain the pseudoinverse and simultaneously obtain insight into the behavior of the scattering operator. A brief review of the SVD of linear operators on Hilbert spaces[15] is given here.

Let A denote a linear operator with kernel $A(x, y)$ which maps the Hilbert space $\mathcal{H}_1$ into the Hilbert space $\mathcal{H}_2$. The SVD of A is a representation of the form

$$A(x, y) = \sum_n \sigma_n g_n(x) f^*_n(y), \quad (33)$$

where σ_n is the singular value associated with the singular functions f_n and g_n. The $\{f_n\}$ and $\{g_n\}$ are orthonormal bases of $\mathcal{H}_1$ and $\mathcal{H}_2$, respectively, and are eigenfunctions with eigenvalues σ_n^2 of the positive self-adjoint operators A^*A and AA^*:

$$A^*Af_n = \sigma_n{}^2 f_n, \tag{34}$$

$$AA^*g_n = \sigma_n{}^2 g_n. \tag{35}$$

In addition the f_n and g_n are related by

$$Af_n = \sigma_n g_n, \tag{36}$$

$$A^*g_n = \sigma_n f_n. \tag{37}$$

The pseudoinverse solution to the equation $Af = g$ is defined to be the minimizer of $\|Af - g\|$ with smallest norm. This well-defined element $f^+ \in N(A)^\perp$ is unique and may be shown[15] to be of the form $f^+ = A^+g$, where the pseudoinverse operator A^+ is given by $A^+ = A^*(AA^*)^{-1}$ and $N(A)^\perp$ is the orthogonal complement of the null space of A. The SVD of A may be used to express A^+ as

$$A^+(x, y) = \sum_n \frac{1}{\sigma_n} f_n(x) g_n^*(y). \tag{38}$$

The SVD approach is next applied to the inverse problem for scalar waves.

A. Scalar Case

The integral Eq. (17) may be rewritten in the form

$$A(\mathbf{q}_1, \mathbf{q}_2) = \int \mathrm{d}^3 r K(\mathbf{q}_1, \mathbf{q}_2;\ \mathbf{r})\eta(\mathbf{r}), \tag{39}$$

where the scattering operator $K(\mathbf{q}_1, \mathbf{q}_2;\ \mathbf{r})$ is given by

$$K(\mathbf{q}_1, \mathbf{q}_2;\ \mathbf{r}) = \exp[i(\mathbf{q}_1 - \mathbf{q}_2)\cdot \boldsymbol{\rho}]\kappa(\mathbf{q}_1, \mathbf{q}_2;\ z), \tag{40}$$

with

$$\kappa(\mathbf{q}_1, \mathbf{q}_2;\ z) = k_0{}^2\{1 + R_1(\mathbf{q}_2)\exp[2ik_z(\mathbf{q}_2)z]\} \times \exp\{i[\mathbf{k}_z(\mathbf{q}_1) - \mathbf{k}_z(\mathbf{q}_2)]z\}. \tag{41}$$

If the transverse range of $\eta(\mathbf{r})$ is contained in the region $[-L, L] \times [-L, L]$, then $\eta(\mathbf{r})$ may be expressed as the Fourier series

$$\eta(\boldsymbol{\rho}, z) = \sum_{\mathbf{q}\in\Lambda} c_{\mathbf{q}}(z)\exp(i\mathbf{q}\cdot\boldsymbol{\rho}), \tag{42}$$

where $c_{\mathbf{q}}(z)$ are appropriate coefficients and $\Lambda = \{(n_x\pi/L, n_y\pi/L): n_x, n_y = 0, \pm 1, \dots\}$. It will prove convenient to allow the transverse wavevectors $\mathbf{q}_1$, $\mathbf{q}_2$ to take values in the discrete set Λ, simplifying the ensuing analysis.

Evidently $A(\mathbf{q}_1, \mathbf{q}_2)$ will not be known for all $\mathbf{q}_1, \mathbf{q}_2 \in \Lambda$. For example the index of refraction n limits $\mathbf{q}_1$, $\mathbf{q}_2$ to the regions $k_0 \le |\mathbf{q}_1| \le nk_0$ and $|\mathbf{q}_2| \le k_0$, respectively. Furthermore, not all $\mathbf{q}_1$, $\mathbf{q}_2$ may be experimentally accessible. It is thus useful to introduce a function $\chi(\mathbf{q}_1, \mathbf{q}_2)$ which is defined to be unity for the $\mathbf{q}_1$, $\mathbf{q}_2$ at which A is measured and zero otherwise. The functions $\kappa(\mathbf{q}_1, \mathbf{q}_2;\ z)$ and $A(\mathbf{q}_1, \mathbf{q}_2)$ are then modified according to $\kappa(\mathbf{q}_1, \mathbf{q}_2;\ z) \to \kappa(\mathbf{q}_1, \mathbf{q}_2;\ z)\chi(\mathbf{q}_1, \mathbf{q}_2)$ and $A(\mathbf{q}_1, \mathbf{q}_2) \to A(\mathbf{q}_1, \mathbf{q}_2)\chi(\mathbf{q}_1, \mathbf{q}_2)$.

To obtain the SVD of $K(\mathbf{q}_1, \mathbf{q}_2;\ \mathbf{r})$ it will prove useful to introduce the identity

$$K(\mathbf{q}_1, \mathbf{q}_2;\ \mathbf{r}) = \sum_{\mathbf{Q}\in\Lambda} \exp(i\mathbf{Q}\cdot\boldsymbol{\rho})\delta(\mathbf{Q} + \mathbf{q}_2 - \mathbf{q}_1) \times \kappa(\mathbf{Q} + \mathbf{q}_2, \mathbf{q}_2;\ z), \tag{43}$$

where δ denotes the Kronecker delta. With this result the matrix elements of the operator KK^* are found to be given by

$$KK^*(\mathbf{q}_1, \mathbf{q}_2;\ \mathbf{q}_1', \mathbf{q}_2') = \sum_{\mathbf{Q}\in\Lambda} M(\mathbf{q}_2, \mathbf{q}_2';\ \mathbf{Q})\delta(\mathbf{Q} + \mathbf{q}_2 - \mathbf{q}_1)\delta(\mathbf{Q} + \mathbf{q}_2' - \mathbf{q}_1'), \tag{44}$$

where

$$M(\mathbf{q}_2, \mathbf{q}_2';\ \mathbf{Q}) = \int_0^L \mathrm{d}z\, \kappa(\mathbf{Q} + \mathbf{q}_2, \mathbf{q}_2;\ z) \times \kappa^*(\mathbf{Q} + \mathbf{q}_2', \mathbf{q}_2';\ z), \tag{45}$$

L being the range of $\eta(\mathbf{r})$ in the $\hat{\mathbf{z}}$ direction. To find the singular vectors $g_{\mathbf{QQ}'}$ of K which satisfy

$$KK^* g_{\mathbf{QQ}'} = \sigma_{\mathbf{QQ}'}{}^2 g_{\mathbf{QQ}'}, \tag{46}$$

it will be useful to make the ansatz

$$g_{\mathbf{QQ}'}(\mathbf{q}_1, \mathbf{q}_2) = C_{\mathbf{Q}'}(\mathbf{q}_2;\ \mathbf{Q})\delta(\mathbf{Q} + \mathbf{q}_2 - \mathbf{q}_1), \tag{47}$$

where $\mathbf{Q}, \mathbf{Q}' \in \Lambda$. Equation (44) now implies that

$$\sum_{\mathbf{q}'\in\Lambda} M(\mathbf{q}, \mathbf{q}';\ \mathbf{Q}) C_{\mathbf{Q}'}(\mathbf{q}';\ \mathbf{Q}) = \sigma_{\mathbf{QQ}'}{}^2 C_{\mathbf{Q}'}(\mathbf{q};\ \mathbf{Q}). \tag{48}$$

Thus $C_{\mathbf{Q}'}(\mathbf{q}_2;\ \mathbf{Q})$ is an eigenvector of $M(\mathbf{Q})$ labeled by $\mathbf{Q}'$ with eigenvalue $\sigma_{\mathbf{QQ}'}{}^2$. Since $M(\mathbf{Q})$ is self-adjoint, the $C_{\mathbf{Q}'}(\mathbf{q}_2;\ \mathbf{Q})$ may be taken to be orthonormal. Next the $f_{\mathbf{QQ}'}$ may be found from $K^* g_{\mathbf{QQ}''} = \sigma_{\mathbf{QQ}'} f_{\mathbf{QQ}'}$, and are given by

$$f_{\mathbf{QQ}'}(\mathbf{r}) = \frac{1}{\sigma_{\mathbf{QQ}'}} \sum_{\mathbf{q}\in\Lambda} \exp(-i\mathbf{Q}\cdot\boldsymbol{\rho})\kappa^*(\mathbf{Q} + \mathbf{q}, \mathbf{q};\ z) C_{\mathbf{Q}'}^*(\mathbf{q};\ \mathbf{Q}). \tag{49}$$

It follows that the SVD of $K(\mathbf{q}_1, \mathbf{q}_2;\ \mathbf{r})$ is given by the expression

$$K(\mathbf{q}_1, \mathbf{q}_2;\ \mathbf{r}) = \sum_{\mathbf{Q},\mathbf{Q}'} \sigma_{\mathbf{QQ}'} f_{\mathbf{QQ}'}^*(\mathbf{r}) g_{\mathbf{QQ}'}(\mathbf{q}_1, \mathbf{q}_2). \tag{50}$$

The SVD of expression (50) may now be used to obtain the pseudoinverse solution to the integral equation (39) as

$$\eta^+(\mathbf{r}) = \sum_{\mathbf{q}_1, \mathbf{q}_2} K^+(\mathbf{r};\ \mathbf{q}_1, \mathbf{q}_2) A(\mathbf{q}_1, \mathbf{q}_2), \tag{51}$$

where $K^+(\mathbf{r};\ \mathbf{q}_1, \mathbf{q}_2)$ is the pseudoinverse of $K(\mathbf{q}_1, \mathbf{q}_2;\ \mathbf{r})$. With the result of Eq. (38), the pseudoinverse K^+ may be seen to be given by

$$K^+(\mathbf{r};\ \mathbf{q}_1, \mathbf{q}_2) = \sum_{\mathbf{Q},\mathbf{Q}'} \frac{1}{\sigma_{\mathbf{QQ}'}} f_{\mathbf{QQ}'}(\mathbf{r}) g_{\mathbf{QQ}'}^*(\mathbf{q}_1, \mathbf{q}_2). \tag{52}$$

Substituting Eqs. (47) and (49) into Eq. (52) and using the spectral decomposition

$$\sum_{\mathbf{Q}'} \frac{1}{\sigma_{\mathbf{QQ}'}{}^2} C_{\mathbf{Q}'}(\mathbf{q};\, \mathbf{Q}) C^*_{\mathbf{Q}'}(\mathbf{q}';\, \mathbf{Q}) = M^{-1}(\mathbf{q},\, \mathbf{q}';\, \mathbf{Q}), \tag{53}$$

where $M^{-1}(\mathbf{q},\, \mathbf{q}';\, \mathbf{Q})$ is the $\mathbf{qq}'$ matrix element of $M^{-1}(\mathbf{Q})$, one obtains

$$\eta^+(\mathbf{r}) = \sum_{\mathbf{q}_1, \mathbf{q}_2, \mathbf{q}_2'} \sum_{\mathbf{Q}} \exp(-i\mathbf{Q} \cdot \boldsymbol{\rho}) \times \delta(\mathbf{Q} + \mathbf{q}_2 - \mathbf{q}_1) M^{-1}(\mathbf{q}_2,\, \mathbf{q}_2';\, \mathbf{Q}) \times \kappa^*(\mathbf{Q} + \mathbf{q}_2',\, \mathbf{q}_2';\, z) A(\mathbf{q}_1,\, \mathbf{q}_2), \tag{54}$$

which is the inversion formula for scalar TIRT.

B. Vector Case

The integral Eq. (31) may be rewritten in the form

$$A_{\alpha\beta}(\mathbf{q}_1,\, \mathbf{q}_2) = \int \mathrm{d}^3 r K_{\alpha\beta}(\mathbf{q}_1,\, \mathbf{q}_2;\, \mathbf{r}) \eta(\mathbf{r}), \tag{55}$$

where the scattering operator $K_{\alpha\beta}(\mathbf{q}_1,\, \mathbf{q}_2;\, \mathbf{r})$ is given by

$$K_{\alpha\beta}(\mathbf{q}_1,\, \mathbf{q}_2;\, \mathbf{r}) = \exp[i(\mathbf{q}_1 - \mathbf{q}_2) \cdot \boldsymbol{\rho}] \kappa_{\alpha\beta}(\mathbf{q}_1,\, \mathbf{q}_2;\, z), \tag{56}$$

$$\kappa_{\alpha\beta}(\mathbf{q}_1,\, \mathbf{q}_2;\, z) = w_{\alpha\beta}(\mathbf{q}_2,\, z) \exp\{i[\mathbf{k}_z(\mathbf{q}_1) - \mathbf{k}_z(\mathbf{q}_2)]z\} \times \chi(\mathbf{q}_1,\, \mathbf{q}_2). \tag{57}$$

As in the scalar case it is assumed that $A(\mathbf{q}_1,\, \mathbf{q}_2)$ is measured for a particular set of $\mathbf{q}_1,\, \mathbf{q}_2$, with the appropriate blocking function $\chi(\mathbf{q}_1,\, \mathbf{q}_2)$. The vector integral [Eq. (55)] differs from its scalar counterpart Eq. (39) only by a factor associated with the polarization. Evidently, when measuring only a fixed component of the scattered field for a particular incident direction, the scalar inversion formula of Eq. (54) may be used to reconstruct $\eta(\mathbf{r})$.

The SVD for the general vector case is next obtained. Following the previous development it may be found that the SVD of $K_{\alpha\beta}(\mathbf{q}_1,\, \mathbf{q}_2;\, \mathbf{r})$ is of the form

$$K_{\alpha\beta}(\mathbf{q}_1,\, \mathbf{q}_2;\, \mathbf{r}) = \sum_{\mathbf{Q},\mathbf{Q}'} \sigma_{\mathbf{QQ}'} f^*_{\mathbf{QQ}'}(\mathbf{r}) g^{\alpha\beta}_{\mathbf{QQ}'}(\mathbf{q}_1,\, \mathbf{q}_2). \tag{58}$$

Here the singular functions are given by

$$g^{\alpha\beta}_{\mathbf{QQ}'}(\mathbf{q}_1,\, \mathbf{q}_2) = C^{\alpha\beta}_{\mathbf{Q}'}(\mathbf{q}_2;\, \mathbf{Q}) \delta(\mathbf{Q} + \mathbf{q}_2 - \mathbf{q}_1), \tag{59}$$

$$f_{\mathbf{QQ}'}(\mathbf{r}) = \frac{1}{\sigma_{\mathbf{QQ}'}} \sum_{\mathbf{q} \in \Lambda} \exp(-i\mathbf{Q} \cdot \boldsymbol{\rho}) \times \kappa^*(\mathbf{Q} + \mathbf{q},\, \mathbf{q};\, z) C^*_{\mathbf{Q}'}(\mathbf{q};\, \mathbf{Q}). \tag{60}$$

The $C^{\alpha\beta}_{\mathbf{Q}'}(\mathbf{q}_2;\, \mathbf{Q})$ are eigenfunctions of $M^{\alpha'\beta'}_{\alpha\beta}(\mathbf{q}_2,\, \mathbf{q}_2';\, \mathbf{Q})$ with eigenvalues $\sigma^2_{\mathbf{QQ}'}$

$$\sum_{\mathbf{q}' \in \Lambda} M^{\alpha'\beta'}_{\alpha\beta}(\mathbf{q},\, \mathbf{q}';\, \mathbf{Q}) C^{\alpha'\beta'}_{\mathbf{Q}'}(\mathbf{q}';\, \mathbf{Q}) = \sigma^2_{\mathbf{QQ}'} C^{\alpha\beta}_{\mathbf{Q}'}(\mathbf{q};\, \mathbf{Q}), \tag{61}$$

where

$$M^{\alpha'\beta'}_{\alpha\beta}(\mathbf{q}_2,\, \mathbf{q}_2';\, \mathbf{Q}) = \int_0^L \mathrm{d}z\, \kappa_{\alpha\beta}(\mathbf{Q} + \mathbf{q}_2,\, \mathbf{q}_2;\, z) \times \kappa^*_{\alpha'\beta'}(\mathbf{Q} + \mathbf{q}_2',\, \mathbf{q}_2';\, z). \tag{62}$$

The pseudoinverse solution to the integral Eq. (55) is given by

$$\eta^+(\mathbf{r}) = \sum_{\mathbf{q}_1, \mathbf{q}_2} K^+_{\alpha\beta}(\mathbf{r};\, \mathbf{q}_1,\, \mathbf{q}_2) A_{\alpha\beta}(\mathbf{q}_1,\, \mathbf{q}_2), \tag{63}$$

where

$$K^+_{\alpha\beta}(\mathbf{r};\, \mathbf{q}_1,\, \mathbf{q}_2) = \sum_{\mathbf{Q},\mathbf{Q}'} \frac{1}{\sigma_{\mathbf{QQ}'}} f_{\mathbf{QQ}'}(\mathbf{r}) g^{\alpha\beta}_{\mathbf{QQ}'}{}^*(\mathbf{q}_1,\, \mathbf{q}_2). \tag{64}$$

More explicitly,

$$\eta^+(\mathbf{r}) = \sum_{\mathbf{q}_1, \mathbf{q}_2, \mathbf{q}_2'} \sum_{\mathbf{Q}} \exp(-i\mathbf{Q} \cdot \boldsymbol{\rho}) \delta(\mathbf{Q} + \mathbf{q}_2 - \mathbf{q}_1) \times [M^{-1}(\mathbf{Q})]^{\alpha'\beta'}_{\alpha\beta}(\mathbf{q}_2,\, \mathbf{q}_2') \kappa^*_{\alpha'\beta'}(\mathbf{Q} + \mathbf{q}_2',\, \mathbf{q}_2';\, z) A_{\alpha\beta}(\mathbf{q}_1,\, \mathbf{q}_2), \tag{65}$$

which is the inversion formula for vector TIRT.

C. Regularization

To avoid numerical instability and to set the resolution of the reconstructed image to be commensurate with the available data, the SVD inversion formulas must be regularized.[15] The effect of regularization is to limit the contribution of the small singular values to the reconstruction. For example, one effective means of regularization is spectral filtering. That is, $1/\sigma^2$ may be replaced in the inversion formulas of Eqs. (53) and (61) by $R(\sigma)$ where R is a suitable filter or regularizer. A reasonable choice for R is the cutoff of all σ below some σ_c. That is $R(\sigma) = \sigma^{-2}\theta(\sigma - \sigma_c)$, θ denoting the usual Heaviside step function. Alternatively a smooth filter, such as that derived by the Tikhonov method, where $R(\sigma) = 1/(\sigma^2 + \sigma_c{}^2)$, may be employed.

4. DISCUSSION

The scattering of evanescent waves into propagating modes by an object of finite extent has been analyzed. It has been demonstrated that in the weak scattering limit where the forward scattering problem may be linearized, an analytic solution of the inverse problem may be obtained. Because the illuminating field is superoscillatory, the object may be reconstructed on subwavelength scales even when the scattered field is measured only in the far zone. The data required to implement this method may be obtained in a TIRM experiment with phase-sensitive measurements of the field. This work thus extends the functionality of TIRM.

Several directions for further research in this area are apparent at this time. First, the sampling scheme described here is general in the sense that any set of points in the data space may be included; however, this method may not always be computationally efficient. That is, the set of available $\mathbf{q}_1$, $\mathbf{q}_2$ may be much smaller than Λ. Specialized sampling schemes with correspondingly recalculated SVDs may be needed. Second, the analysis presented here depends on the prior constraint that the object is of finite extent. There are a number of other prior constraints which may provide some advantage in solving the inverse problem. For instance, the susceptibility may be constrained to be nonnegative, or it may be known that the sample consists only of some particular species or exhibits some known order. Third for some samples the model of single scattering may be inappropriate. For such cases a solution to the nonlinear inverse problem may be required. Finally efforts to implement TIRT experimentally are currently being made.

APPENDIX A

The elements of the tensor $g(q, z)$ are given by

$$g(\mathbf{q}, z) = S^{-1}(\mathbf{q})\tilde{g}(\mathbf{q}, z)S(\mathbf{q}), \tag{A1}$$

where the matrix $S(\mathbf{q})$ rotates $\mathbf{k}(\mathbf{q})$ into the xz plane, $S(\mathbf{q})\mathbf{k}(\mathbf{q}) = [|\mathbf{q}|, 0, k_z(\mathbf{q})]$, or, more explicitly,

$$S(\mathbf{q}) = |\mathbf{q}|^{-1}\begin{bmatrix} q_x & q_y & 0 \\ -q_y & q_x & 0 \\ 0 & 0 & |\mathbf{q}| \end{bmatrix}. \tag{A2}$$

The elements of $\tilde{g}$ are then

$$\tilde{g}_{xx} = \left(\frac{k_z(\mathbf{q})}{k_0}\right)^2 \{1 + R'(\mathbf{q})\exp[2ik_z(\mathbf{q})z']\}, \tag{A3}$$

$$\tilde{g}_{yy} = 1 + R(\mathbf{q})\exp[2ik_z(\mathbf{q})z'], \tag{A4}$$

$$\tilde{g}_{zz} = \left(\frac{|\mathbf{q}|}{k_0}\right)^2 \{1 - R'(\mathbf{q})\exp[2ik_z(\mathbf{q})z']\}, \tag{A5}$$

$$\tilde{g}_{zx} = \frac{-|\mathbf{q}|k_z(\mathbf{q})}{{k_0}^2}\{1 + R'(\mathbf{q})\exp[2ik_z(\mathbf{q})z']\}, \tag{A6}$$

$$\tilde{g}_{xz} = \frac{-|\mathbf{q}|k_z(\mathbf{q})}{{k_0}^2}\{1 - R'(\mathbf{q})\exp[2ik_z(\mathbf{q})z']\}, \tag{A7}$$

all other elements of $\tilde{g}$ being zero; $R(\mathbf{q})$ is defined in Eq. (10), and $R'(\mathbf{q})$ is given by

$$R'(\mathbf{q}) = \frac{k_z'(\mathbf{q}) - nk_z(\mathbf{q})}{k_z'(\mathbf{q}) + nk_z(\mathbf{q})}. \tag{A8}$$

P. S. Carney may be reached at carney@uiuc.edu.

*Present address, Department of Bioengineering, University of Pennsylvania, Philadelphia, Pennsylvania 19104; e-mail, schotland@seas.upenn.edu.

REFERENCES

1. C. W. McCutchen, "Optical systems for observing surface topography by frustrated total internal reflection and interference," Rev. Sci. Instrum. **35**, 1340–1345 (1964).
2. P. A. Temple, "Total internal reflection microscopy: a surface inspection technique," Appl. Opt. **20**, 2656–2664 (1981).
3. P. J. Sides and J. Lo, "Measurement of linear nanometric distances between smooth plane parallel bodies by total internal reflection," Appl. Phys. Lett. **69**, 141–142 (1996).
4. P. T. C. So, H.-S. Kwon, and C. Dong, "Resolution enhancement in standing-wave total internal reflection microscopy: a point-spread-function engineering approach," J. Opt. Soc. Am. A **18**, 2833–2845 (2001).
5. P. S. Carney and J. C. Schotland, "Three-dimensional total internal reflection microscopy," Opt. Lett. **26**, 1072–1074 (2001).
6. D. G. Fischer, "Subwavelength depth resolution in near-field microscopy," Opt. Lett. **25**, 1529–1531 (2000).
7. D. G. Fischer, "The information content of weakly scattered fields: implications for near-field imaging of three-dimensional structures," J. Mod. Opt. **47**, 1359–1374 (2000).
8. A. Lewis, M. Isaacson, A. Harootunian, and A. Muray, "Development of a 500 Å spatial resolution light microscope. I. Light is efficiently transmitted through λ/16 diameter apertures," Ultramicroscopy **13**, 227–231 (1984).
9. D. W. Pohl, W. Denk, and M. Lanz, "Optical stethoscopy: image recording with resolution λ/20," Appl. Phys. Lett. **44**, 651–653 (1984).
10. E. Betzig and J. K. Trautman, "Near-field optics: microscopy, spectroscopy, and surface modification beyond the diffraction limit," Science **257**, 189–195 (1992).
11. R. Dickson, D. Norris, Y.-L. Tzeng, and W. Moerner, "Three-dimensional imaging of single molecules solvated in pores of poly(acrylamide) gels," Science **274**, 966–969 (1996).
12. J.-J. Greffet, A. Sentenac, and R. Carminati, "Surface profile reconstruction using near-field data," Opt. Commun. **116**, 20–24 (1995).
13. P. C. Clemmow, *The Plane Wave Spectrum Representation of Electromagnetic Fields* (Pergamon, Oxford, UK, 1996).
14. A. A. Maradudin and D. L. Mills, "Scattering and absorption of electromagnetic radiation by a semi-infinite medium in the presence of surface roughness," Phys. Rev. B **11**, 1392–1415 (1975).
15. F. Natterer, *The Mathematics of Computerized Tomography* (Wiley, New York, 1986).